Original Article

A comprehensive pan-cancer analysis revealing *SPAG6* as a novel diagnostic, prognostic and immunological biomarker in tumor

Xiaofei Li[1,2,3#^], Yue Wang[4#^], Xiaoyi Li[1,2,3^], Ligang Kong[1,2,3^], Juan J. Díez[5], Haibo Wang[1,2,3^], Daogong Zhang[1,2,3^]

[1]Department of Otolaryngology-Head and Neck Surgery, Shandong Provincial ENT Hospital, Shandong University, Jinan, China; [2]Shandong Provincial Vertigo & Dizziness Medical Center, Jinan, China; [3]Shandong Medical Health Key Laboratory of Vertigo & Vestibular Medicine, Jinan, China; [4]Department of Otorhinolaryngology-Head and Neck Surgery, The First Affiliated Hospital of Ningbo University, Ningbo, China; [5]Department of Endocrinology, Hospital Universitario Puerta de Hierro Majadahonda, Instituto de Investigación Sanitaria Puerta de Hierro Segovia de Arana, Majadahonda, Madrid, Spain

Contributions: (I) Conception and design: Xiaofei Li, D Zhang, H Wang; (II) Administrative support: Xiaofei Li, D Zhang, H Wang; (III) Provision of study materials or patients: Y Wang, Xiaoyi Li; (IV) Collection and assembly of data: Y Wang, Xiaoyi Li; (V) Data analysis and interpretation: Y Wang, L Kong; (VI) Manuscript writing: All authors; (VII) Final approval of manuscript: All authors.

[#]These authors contributed equally to this work as co-first authors.

Correspondence to: Daogong Zhang, PhD; Haibo Wang, MD. Department of Otolaryngology-Head and Neck Surgery, Shandong Provincial ENT Hospital, Shandong University, Jinan, China; Shandong Provincial Vertigo & Dizziness Medical Center, Jinan, China; Shandong Medical Health Key Laboratory of Vertigo & Vestibular Medicine, No. 4, Duanxing West Road, Huaiyin District, Jinan 250000, China. Email: zhangdaogong1978@163.com; whboto11@163.com.

Background: There have been studies on the role of sperm-associated antigen 6 *(SPAG6)* in cytoskeleton formation and growth cone stability, but it is also unknown how spag6 affect tumor growth and development. The aim of this study was to clarify the role of *SPAG6* in pan-cancer, with some findings about thyroid carcinoma (THCA) validated through experiments.

Methods: We examined the role of *SPAG6* in pan-cancer, with the data being collected from databases. Further analysis was conducted to assess its correlations with prognosis, gene heterogeneity, stemness, and tumor immunity. The interacting proteins of *SPAG6* were also identified, and gene ontology enrichment analysis was performed to determine its biological function. We preliminarily confirmed the role of *SPAG6* via *in vitro* experiments and immunofluorescence staining.

Results: This study found that SPAG6 expression was differentially expressed in cancers and at various tumor stages and grades. In stomach and esophageal carcinoma (STES), stomach adenocarcinoma (STAD), kidney renal clear cell carcinoma (KIRC), lung squamous cell carcinoma (LUSC), and adrenocortical carcinoma (ACC), SPAG6 expression was correlated with gender. SPAG6 expression was also found to be correlated with prognostic value, with low expression being associated with poor prognosis. Furthermore, SPAG6 expression was positively linked with immune-related cells in HNSC, chemokine receptors in LUSC, and immune checkpoint genes in THCA. Furthermore, SPAG6 overexpression suppressed the malignant phenotypes of THCA cells, manifested by slower proliferation and decreased migration. The different SPAG6 expression in THCA led to different malignant phenotypes, which are involved in the upregulation of DNA repair, MYC targets, peroxisome, and G2M checkpoint.

Conclusions: *SPAG6* plays a significant role as an oncogene and can be used as a marker to predict the prognosis of cancer. *SPAG6* influences both the tumor immune infiltration and microenvironment, making it a promising immunotherapeutic target for tumor therapy.

^ ORCID: Xiaofei Li, 0000-0001-6968-6256; Yue Wang, 0000-0002-1072-0699; Xiaoyi Li, 0009-0001-2933-1327; Ligang Kong, 0000-0003-1731-2820; Haibo Wang, 0000-0003-0955-9532; Daogong Zhang, 0000-0002-2446-1595.

Keywords: Sperm-associated antigen 6 (SPAG6); pan-cancer; tumor immunity; immune infiltration; tumor microenvironment (TME)

Submitted May 09, 2024. Accepted for publication Jun 21, 2024. Published online Jun 27, 2024.
doi: 10.21037/gs-24-157
View this article at: https://dx.doi.org/10.21037/gs-24-157

Introduction

The tumorigenesis and development of cancers involve complicated changes that result in varying downstream effects. Pan-cancer gene analysis is conducted to identify the similarities and differences among various types of cancer cells (1,2). Cancer-testis antigens (CTAs) have emerged as a promising class of proteins that can stimulate an anticancer immune response (3). CTAs are considered to be novel biomarker, as they are typically only expressed in immune-privileged sites. When expressed in somatic cells, the proteins encoded by these genes elicit both humoral and cell-mediated immune responses, making CTAs highly attractive targets for cancer immunotherapy (4).

Sperm-associated antigen 6 (*SPAG6*), belonging to the CTA family, is essential for microtubule binding and plays a critical role in cytoskeleton formation, growth cone stability, and cilia motility (5-8). Initially identified in human testicular tissue, *SPAG6* governs sperm flagella motility and germ cell maturation (9). Recent investigations have unveiled the association of *SPAG6* with tumorigenesis and progression (10-14). Nonetheless, limited studies have examined the precise mechanisms underlying *SPAG6*'s involvement in cancer and immunity.

The presence of tumor-associated immunogenic proteins poses challenges in developing antigen-specific cancer treatments. Despite the efficacy of tumor immunotherapy, a significant proportion of patients do not benefit. Programmed death 1 (PD-1) is a prominent immune checkpoint receptor (15,16). Dendritic cells (DCs) play a crucial role in antigen presentation and immune response promotion (17). Cancers evade immune recognition through various mechanisms (18). Previous research has linked *SPAG6* to immunodeficiency, which included reduced CD8 cytotoxicity, decreased CD8 T-cell interferon-γ (IFNγ) secretion, and impaired antibody production (19). However, the role of *SPAG6* in thyroid carcinoma (THCA) and other cancers remains unclear.

In this study, we aimed to clarify the relationship between *SPAG6* and multiple cancers by integrating data from multiple databases using polyomics methods. We analyzed the expression, prognosis, gene heterogeneity, and tumor microenvironment (TME) of *SPAG6* and further examined the association between *SPAG6* and immunotherapy across different types of cancers (*Figure 1*). The results of this study provide a comprehensive understanding of the role of *SPAG6* in various types of cancer, and serve as a valuable reference for further research. We present this article in accordance with the MDAR reporting checklist (available at https://gs.amegroups.com/article/view/10.21037/gs-24-157/rc).

Highlight box

Key findings

- *SPAG6* plays a significant role in pan-cancer, especially in thyroid carcinoma (THCA).

What is known and what is new?

- *SPAG6* is a member of the cancer-testis antigen family.
- *SPAG6* is differentially expressed in different cancers, with varying tumor stages and grades, and its expression is also linked to poor prognosis, indicating that it can be used as a marker to predict cancer prognosis.

What is the implication, and what should change now?

- *SPAG6* expression is positively linked with immune-related cells, immunomodulators, and immune checkpoint genes, suggesting its potential as a target for cancer immunotherapy. Spag6 could act as a promising target for cancer treatment and prognostication, especially in THCA.

Methods

Data collection

Data for 34 cancers were downloaded from The Cancer Genome Atlas (TCGA), Therapeutically Applicable Research to Generate Effective Treatment (TARGET), and the Genotype-Tissue Expression (GTEx) databases via the University of California Santa Cruz (UCSC) browser (https://xenabrowser.net/); meanwhile, single-nucleotide

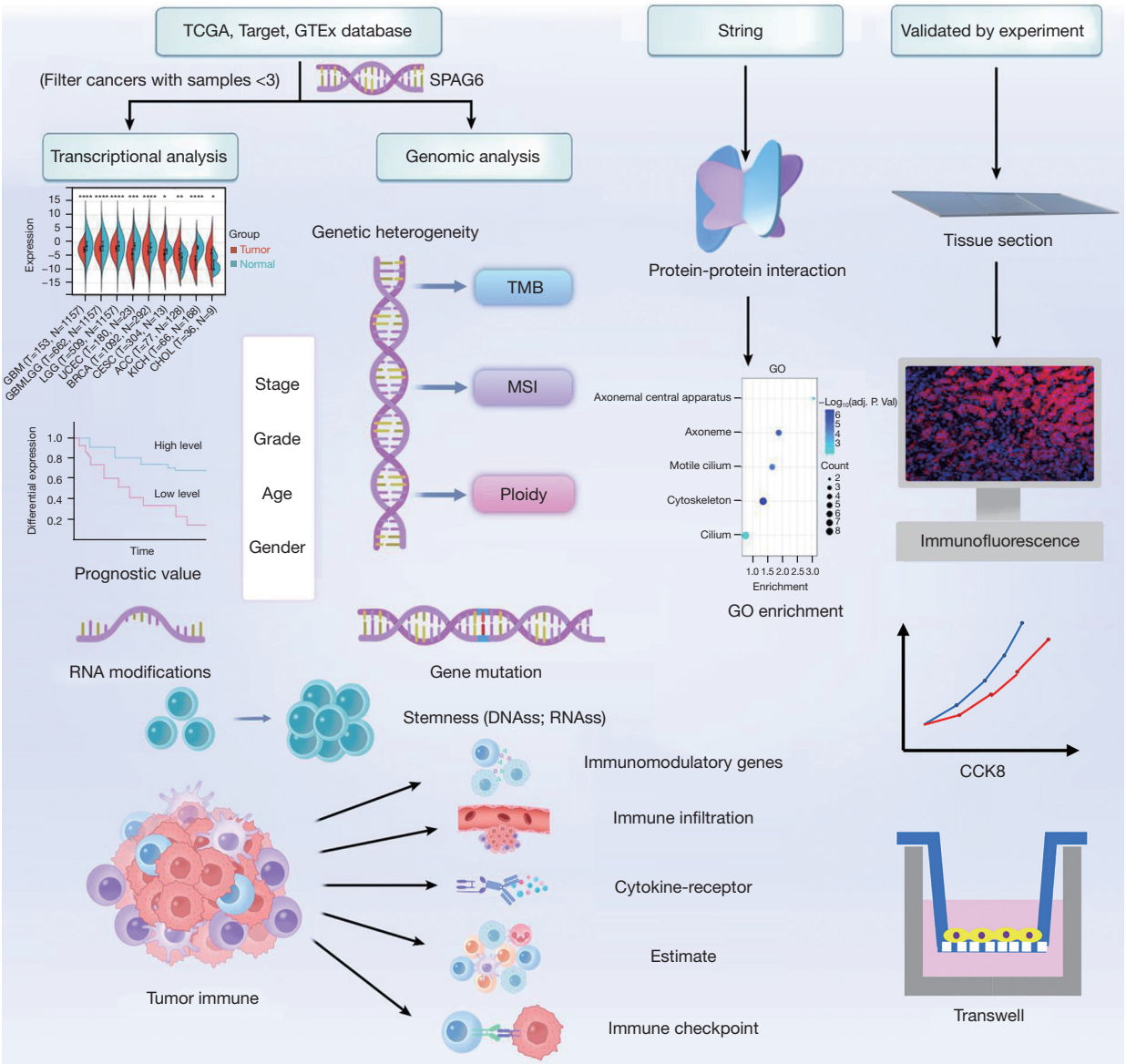

Figure 1 Flowchart of the study. TCGA, The Cancer Genome Atlas; GTEx, Genotype-Tissue Expression; TMB, tumor mutation burden; MSI, microsatellite instability; GO, Gene Ontology; CCK8, Cell Counting Kit 8.

variation data were obtained from the Genomic Data Commons (GDC) portal (https://portal.gdc.cancer.gov/). A list of tumor abbreviations can be found in the Table S1.

SPAG6 expression, pathology, and clinical trait analysis

The expression level of *SPAG6* was analyzed using Posit software, which further integrated information from the databases and a previous study (20). Pearson's correlation method was used to calculate the association between *SPAG6* expression and other factors.

Survival analysis

Kaplan-Meier survival analysis was conducted to assess the disease progression outcome in patients with high or low expression of *SPAG6*. The parameters considered for survival analysis included overall survival (OS), progression-

free interval (PFI), disease-free survival (DFS), and disease-specific survival (DSS). The results were visualized using the "survival" R package (The R Foundation of Statistical Computing), and the Cox proportional hazards regression model was calculated using the coxph function.

Genetic heterogeneity analysis

For the data obtained from TCGA pan-cancer database, Pearson's correlation was used to determine the correlation between *SPAG6* and tumor mutational burden (TMB), microsatellite instability (MSI), tumor ploidy, and tumor purity.

Mutation analysis

R software was used to analyze the expression level of *SPAG6*, with the "maftools" R package being employed to determine the protein structure domains.

Cancer stemness analysis

After collection of pan-cancer data, the expression of *SPAG6* was obtained across various cancer types. Subsequently, messenger RNA (mRNA) expression-based stemness scores (RNAss) and DNA methylation-based stemness scores (DNAss) were obtained (21).

TME and immune-related factor analysis

The "ESTIMATE" R package was used to calculate immune score, stromal score, and ESTIMATE score. The "IOBR" R package was used to estimate *SPAG6* gene expression data (22). The Tumor Immune Estimation Resource (TIMER; cistrome.shinyapps.io/timer) platform was used to determine the correlation of *SPAG6* expression with immune infiltration factors (23). Pearson correlation coefficients were calculated using the corr.test function in the "psych" R package for tumor scores and immunomodulators (24).

Protein-protein interaction network construction and enrichment analysis

The Search Tool for the Retrieval of Interacting Genes/Proteins (STRING) database (https://string-db.org/) was accessed for hub targets and to conduct Gene Ontology (GO) enrichment analysis using parameters "medium" (≥0.4) and "Homo sapiens". Results were visualized using Bioinformatics (http://www.bioinformatics.com.cn/). Adjusted P values were calculated using the false discovery rate (FDR) algorithm for result filtering. Gene set enrichment analysis (GSEA) was conducted with GSEA software (version 3.0) from the GSEA website (http://software.broadinstitute.org/gsea/index.jsp). The *SPAG6* high-expression group (≥50%) and low-expression group (<50%) were defined. Gene analysis was conducted using h.all.v7.4. symbols.gmt in GSEA software with a minimum gene set of 5 and a maximum gene set of 5,000.

Immunohistochemical staining

The tissues samples were obtained from the patients with liver hepatocellular carcinoma (LIHC), cholangiocarcinoma (CHOL), ovarian serous cystadenocarcinoma (OV), uterine corpus endometrial carcinoma (UCEC), cervical squamous cell carcinoma and endocervical adenocarcinoma (CESC), or THCA from pathology department, Shandong Provincial ENT Hospital, between September 2021 to February 2024. Formalin-fixed tissue sections from various cancers were fully embedded and cut into 10 μm sections for immunohistochemical staining. After dewaxing and antigen retrieval, the sections were blocked with PBT-1 for 60 minutes at room temperature. The sections were then incubated overnight with a primary antibody against spag6 (anti-SPAG6, 1:200, ab155653, Abcam, Cambridge, MA, USA) at 4 ℃. Subsequently, a secondary antibody conjugated with Alexa Fluor 546 (1:1,000, Invitrogen, Carlsbad, CA, USA) and DAPI (1:1,000, D9542, Sigma-Aldrich, St. Louis, MO, USA) were incubated for 1 hour at room temperature. The sections were washed with buffer at each step. The final staining was visualized using a laser scanning confocal microscope (Leica SP8, Leica, Wetzlar, Germany).

Cell transfection

PEIpro (Polyplus) was applied for conducting cell transfection, which lasted 48 hours as per its standard guide. B-CPAP, and KTC-1 cells (Stem Cell Bank, Chinese Academy of Sciences; American Type Culture Collection) were transfected with *SPAG6*-overexpressed plasmid or

empty vector as a negative control by GeneChem.

Cell Counting Kit 8 assay (CCK8)

B-CPAP, and KTC-1 cells were processed as required and seeded into 96-well plates at a density of [3–5]×10^3 per well. After treatment for 0, 24, 48, 72 and 96 h, 10 µL CCK8 (BioSharp, Anhui, China) was added to each well, and absorbance was measured at 450 nm with a spectrophotometer after incubation for 2 h.

Transwell migration assays

Cell migration was assessed using an 8-µm Transwell chamber (BioSharp, Anhui, China). Serum-free 1640 medium (200 µL) containing 4×10^4 cells were seeded in the upper chamber. 500 µL 1640 medium containing 20% FBS was added to the lower chamber. After incubation for 24 h, the cells were fixed with 4% paraformaldehyde and stained with 0.1% crystal violet. Migrated cells were photographed in four random fields using an inverted light microscope (Olympus, Tokyo, Japan). The experiments were repeated three times independently. Data were quantified via the ImageJ software.

Statistical analysis

Data were $\log_2$ transformed. The Wilcoxon rank-sum and signed-rank tests were used to compare two groups, while the Kruskal-Wallis test was used to compare multiple groups, and the logrank test was used for survival analysis. Significance was defined as a P value <0.05. Pearson correlation coefficient was used to analyze the correlation of *SPAG6* expression with other factors.

Ethical statement

The studies involving human samples were approved by the Shandong Provincial ENT Hospital Ethical Committee (No. 2024-019-01). Written informed consent to participate in this study was provided by the participants. The study was conducted in accordance with the Declaration of Helsinki (as revised in 2013).

Results

Clinical landscape of SPAG6 expression in pan-cancer

The analysis revealed that *SPAG6* expression was upregulated in 11 cancers [kidney renal papillary cell carcinoma (KIRP), LIHC, high-risk Wilms tumor (WT), OV, pancreatic adenocarcinoma (PAAD), uterine carcinosarcoma (UCS), acute lymphoblastic leukemia (ALL), acute myeloid leukemia (LAML), pheochromocytoma and paraganglioma (PCPG), adrenocortical carcinoma (ACC), and CHOL] and downregulated in 17 cancers [glioblastoma multiforme (GBM), glioma (GBMLGG), brain lower-grade glioma (LGG), UCEC, breast invasive carcinoma (BRCA), CESC, lung adenocarcinoma (LUAD), pankidney cohort (KIPAN), colon adenocarcinoma (COAD), colon adenocarcinoma/rectum adenocarcinoma esophageal carcinoma (COADREAD), kidney renal clear cell carcinoma (KIRC), lung squamous cell carcinoma (LUSC), skin cutaneous melanoma (SKCM), THCA, rectum adenocarcinoma (READ), testicular germ cell tumors (TGCT), and kidney chromophobe (KICH)] (*Figure 2A*). Tumor stage showed a correlation with *SPAG6* expression in seven cancers (KIRP, KIPAN, UCEC, LUSC, OV, TGCT, and UCS) (*Figure 2B*). Gender-based differences in *SPAG6* expression were observed in five cancers, with higher expression in male patients in the stomach and esophageal carcinoma (STES), stomach adenocarcinoma (STAD), KIRC, and LUSC and higher expression in female patients in ACC (*Figure 2C*). *SPAG6* expression also varied with tumor grade in seven cancers [GBMLGG, LGG, CESC, STES, STAD, head and neck squamous cell carcinoma (HNSC), and LIHC] (*Figure 2D*). Age-based differences in *SPAG6* expression were found in six cancers, with a positive association in thymoma (THYM) and TGCT and a negative association in GBMLGG, CESC, KIRP, and prostate adenocarcinoma (PRAD) (*Figure 2E*).

Prognostic value of SPAG6 across cancers

Cox regression analysis revealed a correlation between *SPAG6* expression and five cancer types. High *SPAG6* expression was associated with poor prognosis in LAML, ALL, and lymphoid neoplasm diffuse large b-cell lymphoma (DLBC), while low expression was associated with poor prognosis in PAAD and TGCT (*Figure 3A*). Kaplan-Meier curves further confirmed the impact of *SPAG6* expression on osteosarcoma (OS), with high expression associated with poor prognosis in LAML, ALL, and DLBC (*Figure 3B-3D*) and low expression associated with poor prognosis in PAAD and TGCT (*Figure 3E,3F*). Additionally, *SPAG6* expression correlated with DSS in LIHC, DLBC, KIRP, KIPAN, and bladder urothelial carcinoma (BLCA). High *SPAG6*

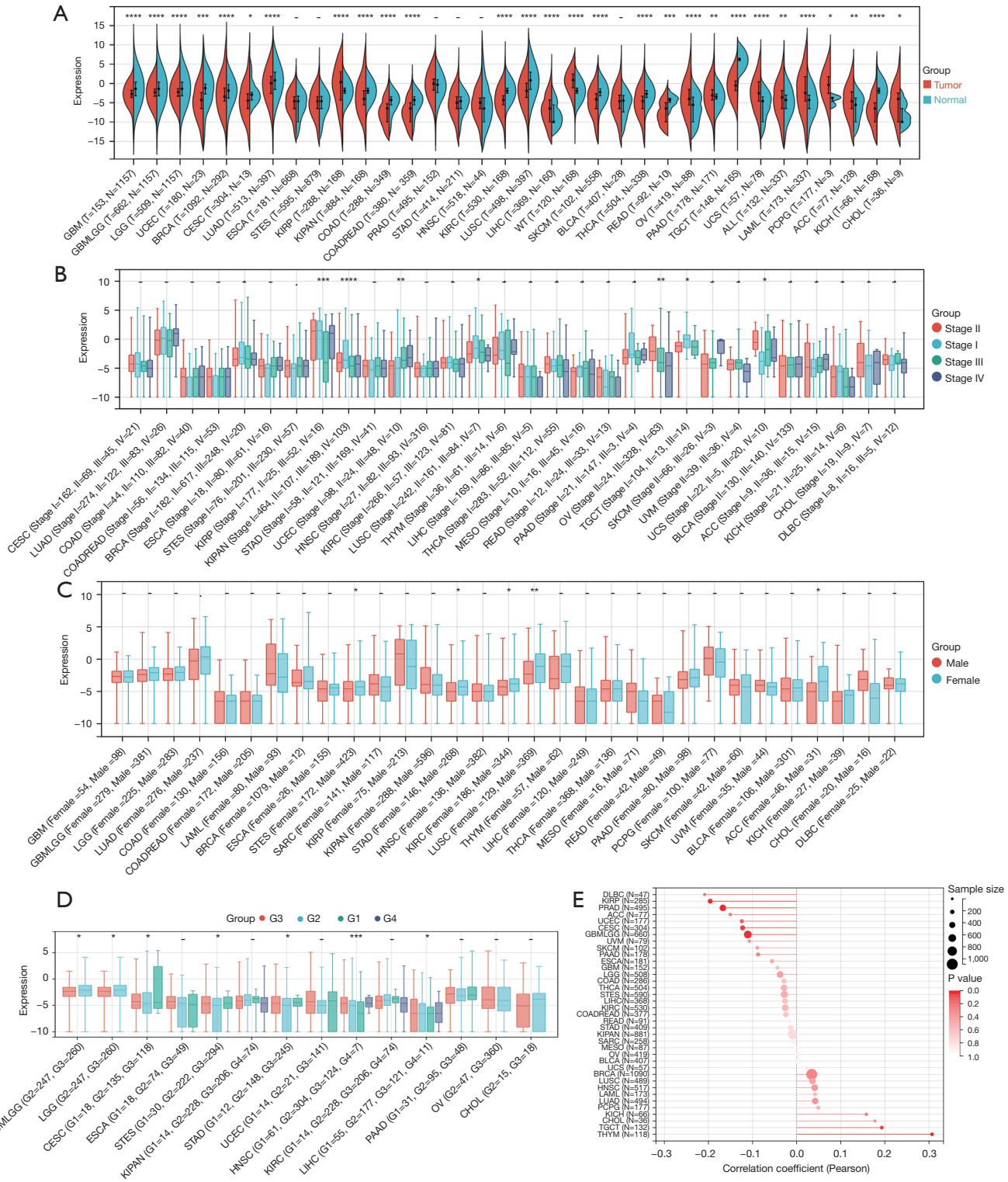

Figure 2 Expression of *SPAG6* in the clinical data. (A) The differential expression of *SPAG6* in pan-cancer (red) and normal tissues (blue) downloaded from different databases. (B) The correlation between tumor stage and *SPAG6* expression. Stage I = blue, stage II = red, stage III = green, and stage IV = purple. (C) The correlation between patients' gender and *SPAG6* expression. Male = red and female = blue. (D) The correlation between patients' grade and *SPAG6* expression. Grade 1 = green, grade 2 = blue, grade 3 = red, and grade 4 = purple. (E) The correlation between patients' age and *SPAG6* expression. –, no statistical significance; *, P<0.05; **, P<0.01; ***, P<0.001; ****, P<0.0001. G, grade.

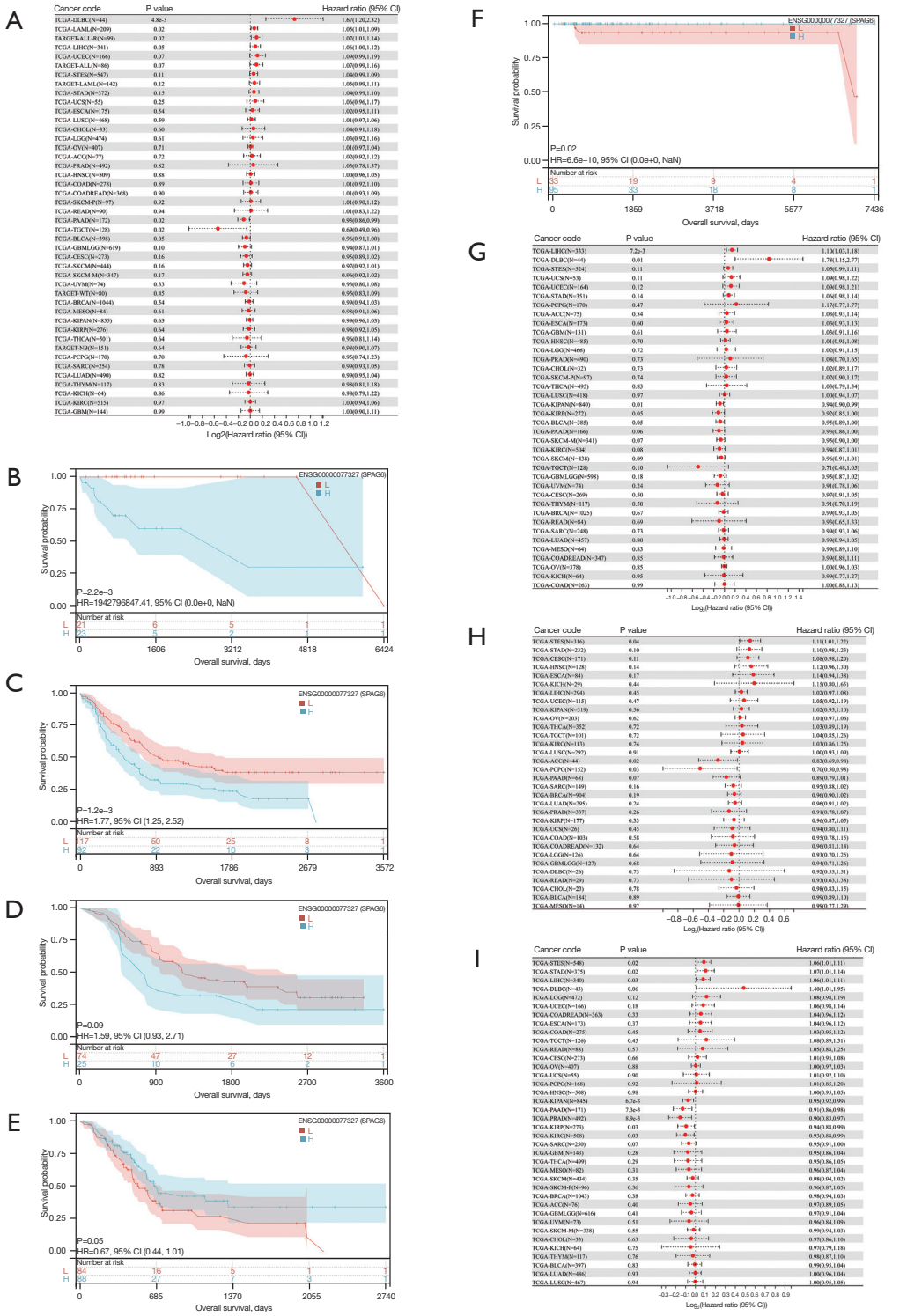

Figure 3 Prognostic value of *SPAG6* across cancers. (A) The correlation between OS and *SPAG6* expression. (B-F) Kaplan-Meier analysis of significant outcomes in OS, namely DLBC, LAML, ALL, PAAD, and TGCT. (G) The correlation between DSS and *SPAG6* expression. (H) The correlation between DFI and *SPAG6* expression. (I) The correlation between PFI and *SPAG6* expression. HR, hazard ratio; CI, confidence interval; NaN, not a number; L, low; H, high; OS, overall survival; DLBC, lymphoid neoplasm diffuse large b-cell lymphoma; LAML, acute myeloid leukemia; ALL, acute lymphoblastic leukemia; PAAD, pancreatic adenocarcinoma; TGCT, testicular germ cell tumor; DSS, disease-specific survival; DFI, disease-free interval; PFI, progression-free interval.

expression correlated with poor prognosis in LIHC and DLBC, while low expression correlated with poor prognosis in KIRP, KIPAN, and BLCA (*Figure 3G*). The analysis also indicated a relationship between *SPAG6* expression and DFI in three cancers (*Figure 3H*), with high expression correlating with poor prognosis in STES and low expression correlating with poor prognosis in PCPG and ACC. *SPAG6* expression correlated with PFI in eight cancers (*Figure 3I*), with high expression correlating with poor prognosis in STES, STAD, and LIHC and low expression correlating with poor prognosis in KIRP, KIPAN, PRAD, KIRC, and PAAD.

Correlation between SPAG6 expression and genetic heterogeneity

Our analysis revealed a correlation between *SPAG6* expression and TMB (*Figure 4A*). Positive correlations between *SPAG6* expression and TMB were observed in GBMLGG, TGCT, and BLCA, while negative correlations were found in esophageal carcinoma (ESCA), STES, STAD, LUSC, and UCS. Similarly, the correlation between *SPAG6* expression and MSI was analyzed *(Figure 4B*). Positive relationships were observed in GBMLGG, LGG, and KIRC, while negative relationships were found in ESCA, STES, UCEC, and LUSC. Furthermore, the correlation between *SPAG6* expression and tumor ploidy was analyzed (*Figure 4C*). Positive associations were found in UCEC, OV, TGCT, and BLCA, while negative associations were observed in BRCA, HNSC, and THYM.

Correlation between SPAG6 expression and gene mutation

The box plot (*Figure 4D*) revealed a striking difference in *SPAG6* mutation between HNSC and BLCA. To gain a deeper understanding of *SPAG6* gene mutations, we analyzed level 4 samples from TCGA and obtained the mutation status of SPAG6 protein's structural domain in various cancer types (*Figure 4E*).

Relationship of SPAG6 expression and RNA modifications

We examined the association between 41 cancer types and three RNA regulators (m1A, m5C, and m6A) (*Figure 4F*). The heatmap depicted methyltransferases to be "writers", demethylases to be "erasers", and binding proteins to be "readers". The results revealed a negative correlation between *SPAG6* and most RNA regulators in LGG and GBMLGG, while a positive correlation was observed in KIPAN, KIRP, LIHC, OV, neuroblastoma (NB), UCEC, KIRC, and BLCA for most RNA modifications.

Analysis of SPAG6 expression and TME

The TME is a complex milieu comprising diverse cell types that can either facilitate or impede tumor growth (1,25). The diagram depicted a significant correlation between *SPAG6* expression and tumor purity in 16 cancer types (*Figure 5A*). In KIPAN, high *SPAG6* expression was associated with high tumor purity, while the opposite trend was observed in the remaining 15 cancer types, including GBM, GBMLGG, LGG, LUAD, COAD, COADREAD, ESCA, STES, STAD, PRAD, LUSC, THCA, READ, BLCA, and DLBC.

We then investigated the association between *SPAG6* activity and immune infiltration by calculating immune score, stromal score, and ESTIMATE score in pan-cancer. In the majority of the 44 cancers analyzed, all 3 scores exhibited a positive association with *SPAG6* expression. Interestingly, *SPAG6* expression was positively associated with the 3 scores in 13 cancers, including COAD, COADREAD, ESCA, GBM, HNSC, LGG, LUAD, LUSC, READ, SKCM, SKCM-M, STAD, and STES, but was negatively associated in KIPAN and OV. The cancers with the lowest P value in each score for ESTIMATE score, immune score, and stromal score are presented in *Figure 5B-5D*, *Figure 5E-5G*, and *Figure 5H-5J*, respectively.

Furthermore, the results showed a significant positive correlation between immune-related cells and almost cancers, except for DLBC and UCS. *Figure 5K* shows that all six immune-related cells were positively associated with *SPAG6* expression in HNSC, LGG, COADREAD, LUSC, COAD, and THCA. These results were consistent with those of the three tumor immune scores.

The result also showed that *SPAG6* expression and was positively correlated with immunomodulators in various cancers. In HNSC, it showed positive associations with most chemokines, but it was negatively correlated to nearly a quarter of the chemokines in KIPAN (*Figure 5L*). In LUSC, *SPAG6* expression was positively correlated with almost all types of chemokine receptors, with no negative correlation observed. We also found a clear positive association between *SPAG6* expression and immune inhibitors in HNSC, LUAD, and STES but a negative association with PDCD1LG2 in THYM. Additionally, a positive association was found between *SPAG6* expression

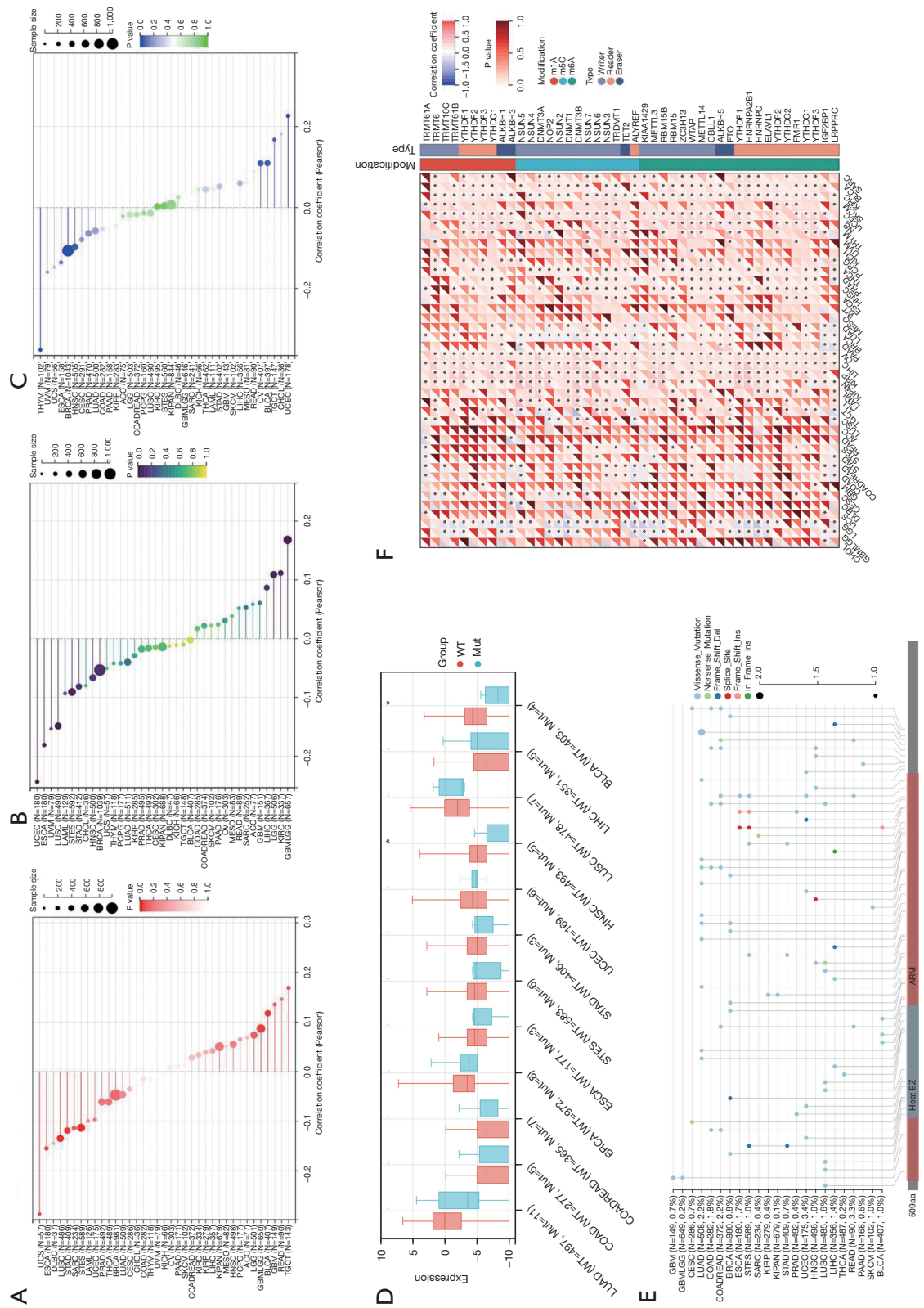

Figure 4 The expression of *SPAG6* was associated with heterogeneity, gene mutation, and RNA modifications. (A-C) The lollipop plots indicate that *SPAG6* was associated with genetic heterogeneity, namely TMB (A), MSI (B), and tumor ploidy (C). (D) The correlation between *SPAG6* and gene mutation. Wild type = red and mutation = blue. (E) The landscape of the single-nucleotide variants of *SPAG6*. (F) The correlation between RNA modifications and *SPAG6* expression. –, no statistical significance; *, P<0.05. WT, wild type; Mut, mutant; TMB, tumor mutational burden; MSI, microsatellite instability.

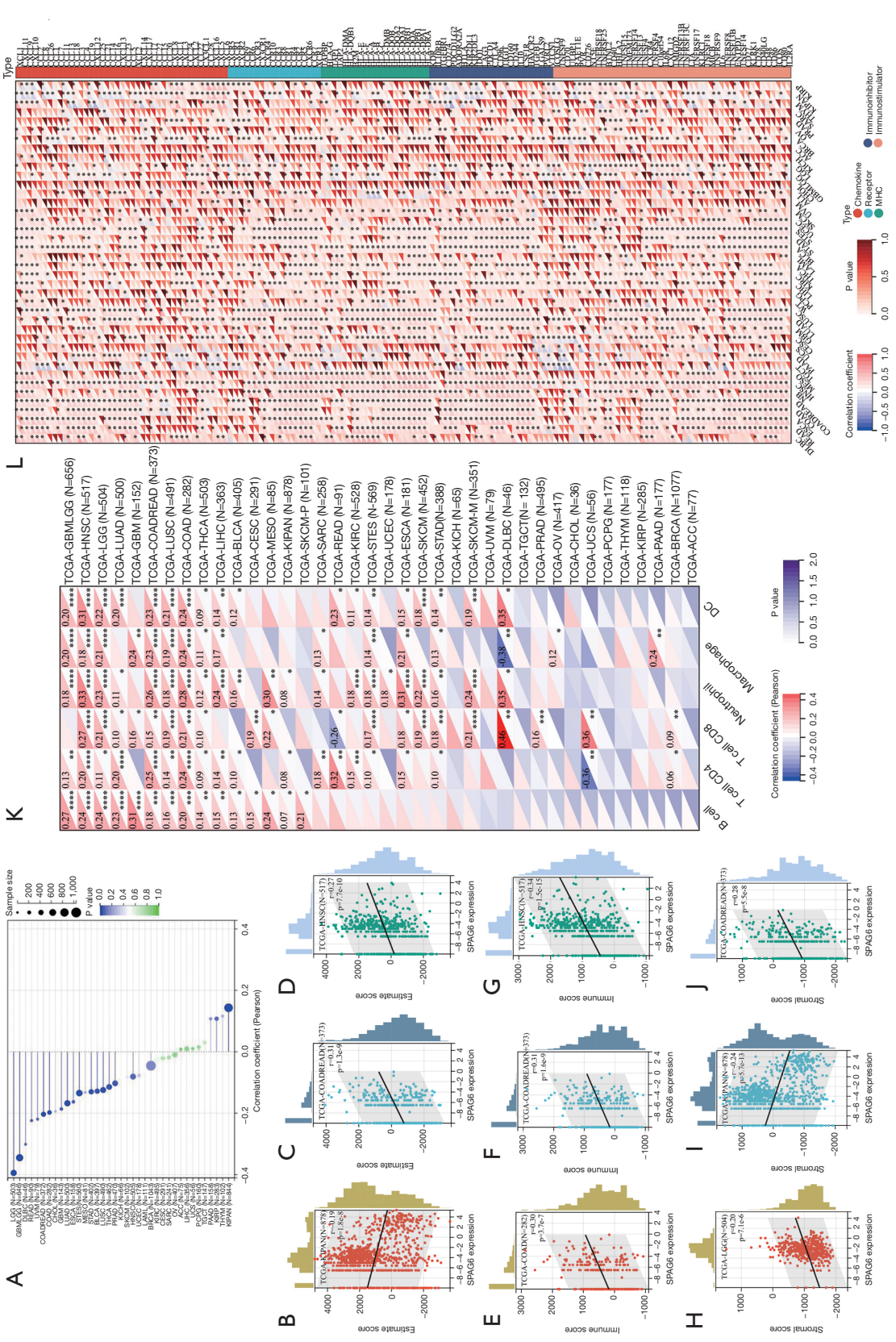

Figure 5 The association between *SPAG6* and tumor-related immunity in the tumor microenvironment. The correlation between tumor purity and *SPAG6* expression. (A-D) The correlation between *SPAG6* and infiltration as calculated by ESTIMATE score. (E-G) The correlation between *SPAG6* and infiltration as calculated by immune score. (H-J) The correlation between *SPAG6* and infiltration as calculated by stromal score. (K) The correlation between immune-related cells and *SPAG6* expression. (L) The correlation between immunomodulators and *SPAG6* expression. *, P<0.05; **, P<0.01; ***, P<0.001; ****, P<0.0001. DC, dendritic cell; MHC, major histocompatibility complex.

and immunostimulators in HNSC and a negative association with TGCT. Notably, *SPAG6* expression was positively correlated with all detected major histocompatibility complex (MHC) molecules in HNSC. In contrast, *SPAG6* expression in ALL demonstrated a negative correlation with several types of MHC.

The role of SPAG6 in cancer stemness

Cancer stem cells, characterized by self-renewal abilities, contribute critically to tumor initiation, progression, and metastasis (26). *SPAG6* expression exhibited negative associations with DNAss and RNAss in cancers, except for LGG, PRAD, LIHC, and TGCT, where a positive correlation was observed with DNAss (*Figure 6A*). Additionally, LIHC, OV, PCPG, and BLCA showed a positive correlation with *SPAG6* expression and RNAss (*Figure 6B*).

Correlation between SPAG6 expression and immune checkpoint genes

The analysis included 60 immune checkpoint genes (*Figure 6C*), and *SPAG6* expression showed a strong positive correlation with several genes in multiple cancers, such as READ, NB, COAD, COADREAD, STAD, STES, LUAD, KIRC, and THCA. Conversely, negative associations were observed with genes such as GBMLGG, LGG, KIRP, and KIRP. This suggests that *SPAG6* has a significant role as a potential target for immunotherapy in various cancers. However, negative immunological associations were found with certain immune inhibitory genes (e.g., *VEGFA*, *CD274*) and immune stimulatory genes (e.g., *TNFRSF4*, *CXCL10*), indicating that elevated *SPAG6* expression levels might hinder the efficacy of therapy in tumors.

GO enrichment analysis based on the protein-protein interaction network

The results indicate that the top 10 proteins with the strongest interactions with SPAG6 were CFAP221, SPAG16, MEIG1, SPAG17, DAW1, TEKT1, CAPZA3, EFHC1, WDR16, and CSE1L (*Figure 6D*). The top five most enriched biological processes (BPs) were the axonemal central apparatus, axoneme, motile cilium, cytoskeleton, and cilium (*Figure 6E*).

SPAG6 overexpression suppressed proliferation, migration, and invasion of THCA cell lines

Immunofluorescence staining demonstrated high SPAG6 expression in LIHC, CHOL, and OV tumor samples and a low expression in UCEC, CESC, and THCA (*Figure 7A*). There exist distinct pathological subtypes within THCA, each characterized by unique etiopathogenic and clinical perspectives. Papillary THCA arises from the follicular thyroid cells, representing the predominant subtype, constituting over 80% of THCA cases. B-CPAP cells and KTC-1 cells are two common types of cell lines for studying THCA. Notably, KTC-1 cells are utilized in research involving human thyroid cancer, while B-CPAP cells also serve as a model for studying human thyroid cancer, especially for papillary THCA. Then, further investigation focused on the potential role of *SPAG6* in THCA. Overexpression of *SPAG6* in THCA cell lines resulted in decreased proliferation and migration ability, as observed in the CCK8 assay and Transwell migration assay, respectively (*Figure 7B*,*7C*). These experimental results validated the findings from the bioinformatics analysis.

The expression of *SPAG6* was lower in tumor samples compared to normal samples. The prognostic value of *SPAG6* in THCA varied (*Figure 8A*), with high expression being associated with high PFI and low expression being associated with high DFI (*Figure 8B*,*8C*). Low *SPAG6* expression indicated a lower risk of THCA and tumor recurrence but a higher risk of death from nonneoplastic causes. Mutational analysis revealed frequent *BRAF* (–) gene mutations in both the *SPAG6* high- and low-expression groups, with distinct mutations in the *SPTA1* gene for the high expression group and the *VPS13A* gene for the low expression group (*Figure 8D*). GSEA revealed distinct signaling pathways associated with high and low *SPAG6* expression, including DNA repair, MYC targets, peroxisome, and G2M checkpoint, which could explain the observed clinical outcomes (*Figure 8E-8H*).

Discussion

In this comprehensive study, we analyzed *SPAG6* expression across 34 different cancers using multiple databases. Our findings support previous research (5,6,27), indicating that *SPAG6* is upregulated in 11 cancers and downregulated in

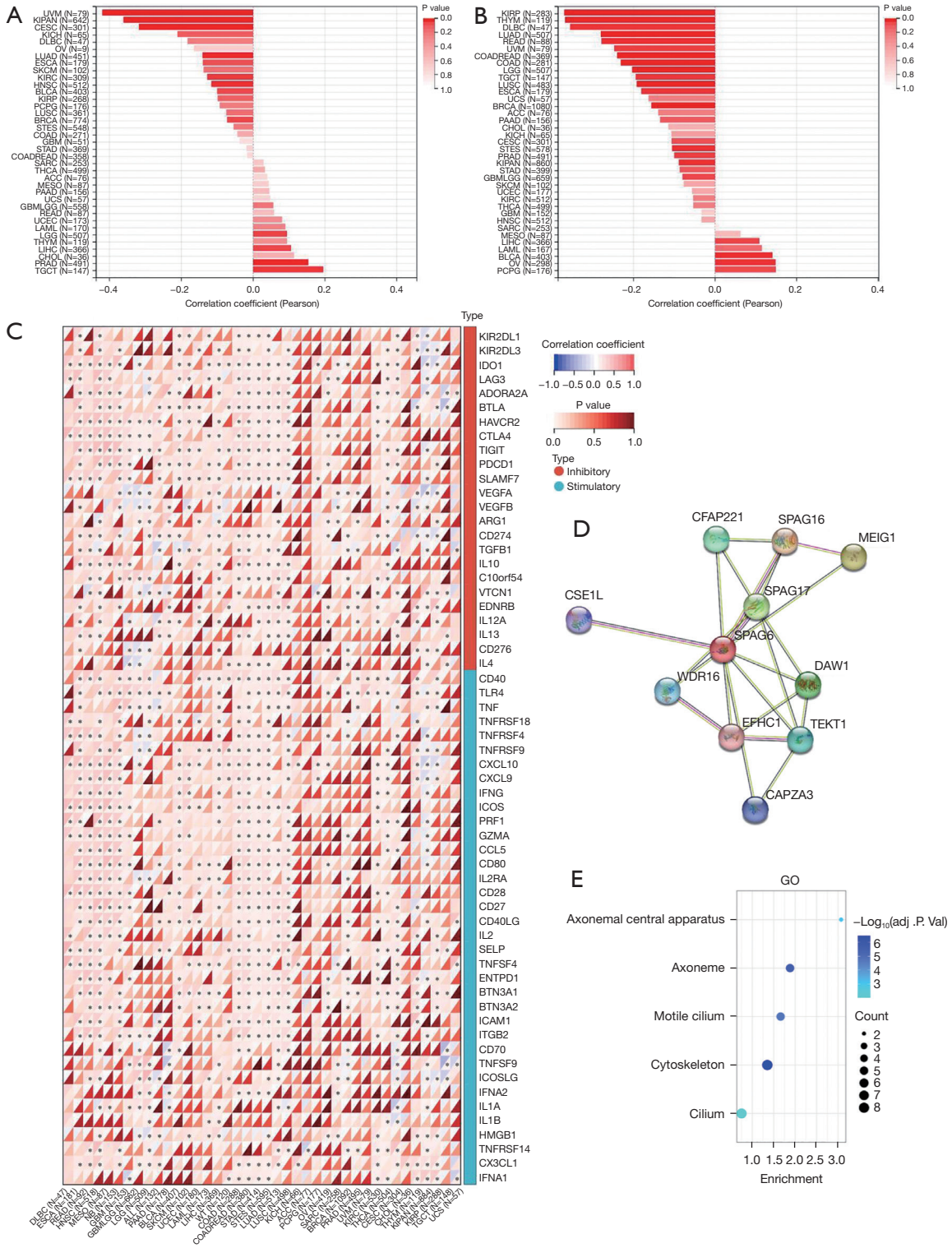

Figure 6 Correlation of *SPAG6* expression as tumor stemness and immune checkpoint genes and the enrichment analysis its interacting targets. (A,B) The association between *SPAG6* expression and tumor stemness, including DNAss (A) and RNAss (B). (C) The association between *SPAG6* expression and immune checkpoints in pan-cancer. (D) The protein-protein interaction network of *SPAG6*. (E) The Gene Ontology enrichment analysis of *SPAG6* and its interacting targets. *, P<0.05. GO, Gene Ontology.

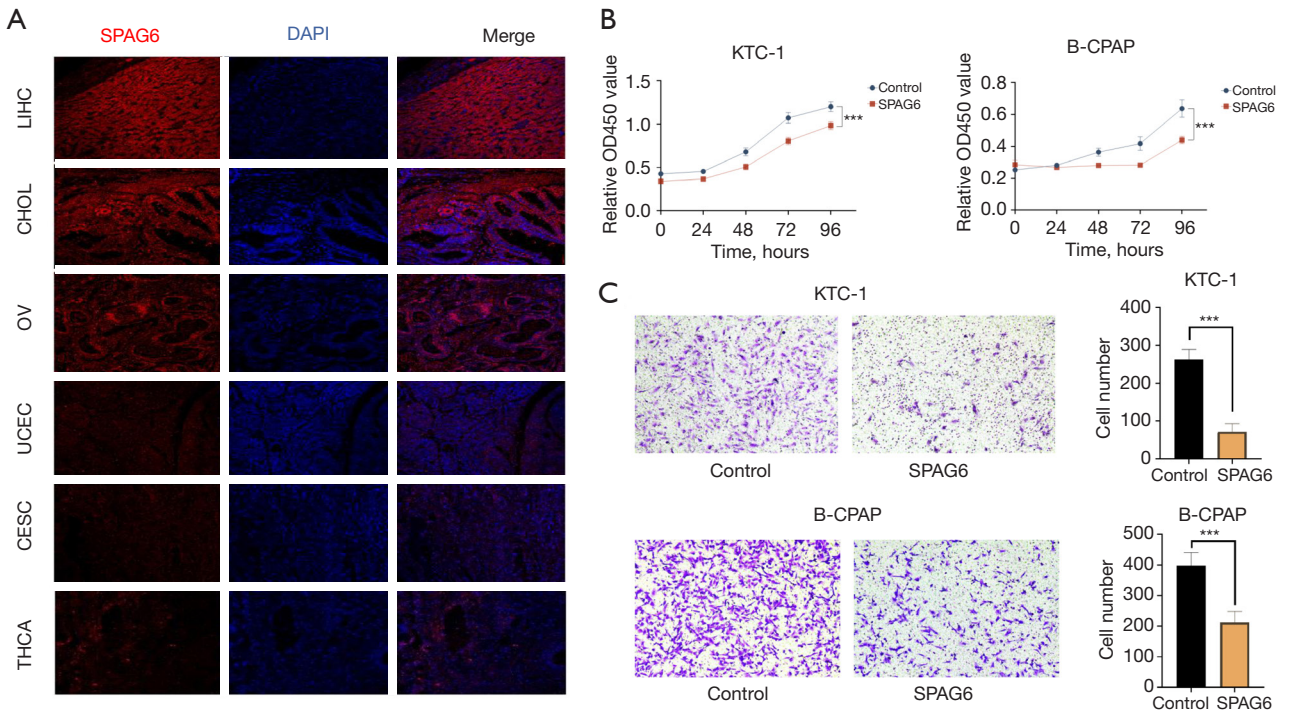

Figure 7 Experimental validation of SPAG6 expression. (A) Multiple immunofluorescence staining of SPAG6 in pan-cancer tissue sections. Views of cancers, including high expression (LIHC, CHOL, and OV) and low expression (UCEC, CESC, and THCA) under microscopy (200×). SPAG6 = red, cellular nuclei = blue (DAPI). (B) Cell Counting Kit 8 assay of *SPAG6*. (C) Transwell migration assay of *SPAG6* (10× magnification). The cells were fixed with 4% paraformaldehyde and stained with 0.1% crystal violet. Migrated cells were photographed with a microscope. ***, P<0.001. LIHC, liver hepatocellular carcinoma; CHOL, cholangiocarcinoma; OV, ovarian serous cystadenocarcinoma; UCEC, uterine corpus endometrial carcinoma; CESC, cervical squamous cell carcinoma and endocervical adenocarcinoma; THCA, thyroid carcinoma; DAPI, 4,6-diamidino-2-phenyiindole 2 hci.

17 cancers. In this study, we focused on the high incidence of thyroid cancer and conducted *in vitro* experiments to preliminarily confirm the possible role of spag6 in cancer. The expression of *SPAG6* was downregulated in THCA and was associated with prognosis. The differential expression of *SPAG6* regulates especially proliferation and metastasis in THCA. In thyroid cancer with *SPAG6* expression, its expression is associated with immune cell infiltration. Additionally, the expression of immune checkpoints shows a strong correlation with *SPAG6*. When *SPAG6* expression is low, the risk of THCA tumor recurrence is lower, but the risk of death from non-tumor causes is relatively higher. Therefore, for the treatment and prognosis evaluation of THCA, *SPAG6* expression may be an important target. The relationships found between the expression of SPAG6 and the cells of the immune system may be of interest from a clinical point of view. Immunotherapy currently has limited clinical application in advanced thyroid cancer. The use of pembrolizumab (28), a PD-1 inhibitor, and the combination of the CTLA-4 inhibitor ipilimumab with the PD-1 inhibitor nivolumab have been tested (29). In all cases clinical efficacy has been poor. The results of the present study open a new potential avenue of action against thyroid cancer through the immune system. A study has suggested that gene fusion can lead to upregulation of *SPAG6*, as observed in leukemia samples (30). Additionally, silencing of *SPAG6* expression has been linked to apoptosis and differentiation of leukemia cells through the PI3K–AKT signaling pathway (31). These results provide preliminary insight into the role of *SPAG6* in cancer initiation and progression.

Our study suggests that *SPAG6* expression was associated with certain clinical characteristics of malignant tumors. Additionally, the combination of *SPAG6* with other markers has been proposed as a promising biomarker for early breast cancer diagnosis via a liquid biopsy approach (32).

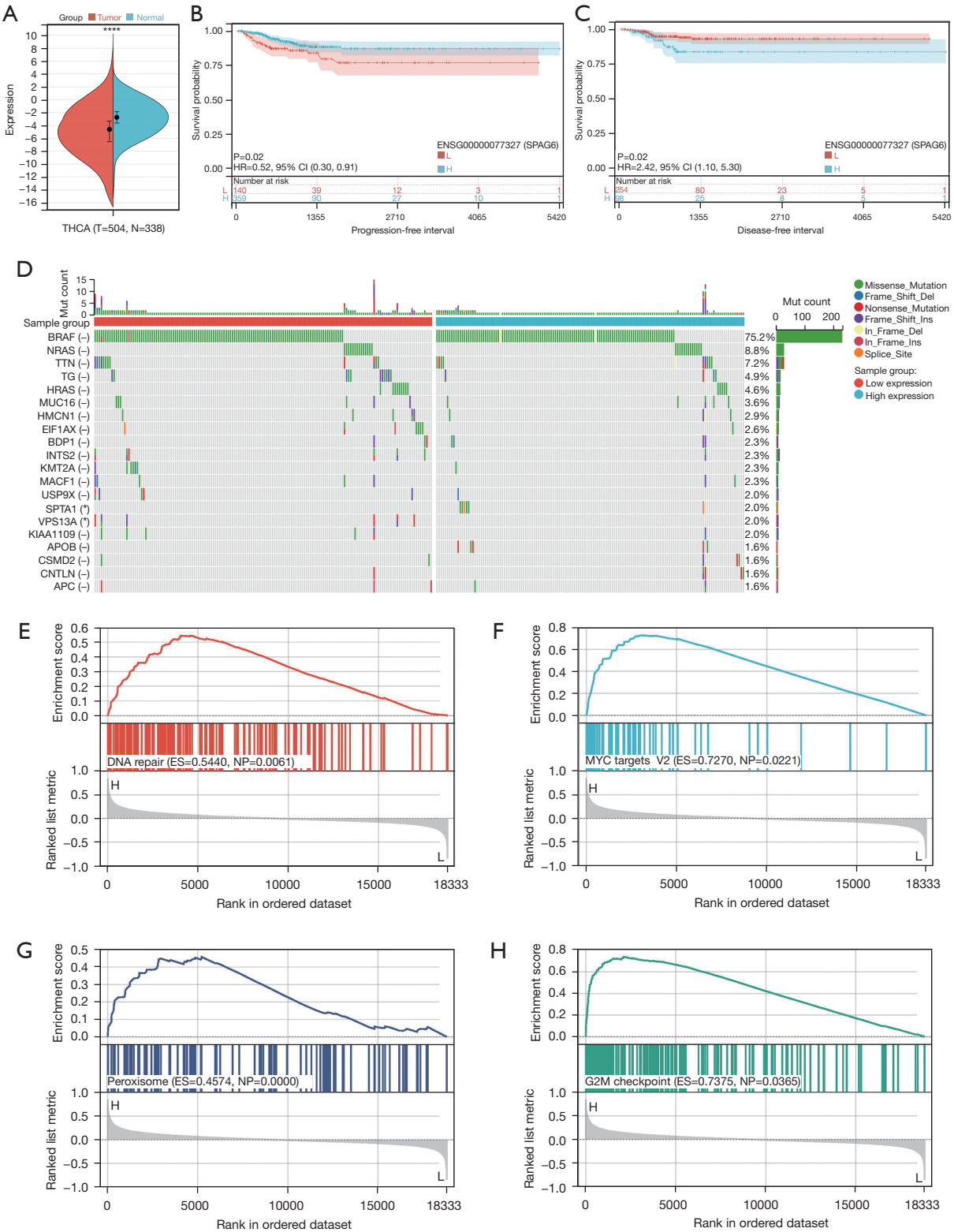

Figure 8 The effect of *SPAG6* overexpression on the THCA cell lines. (A) Differential expression of *SPAG6* in normal and tumor tissues. (B,C) Prognostic value of SPAG6 in THCA. (D) Mutated genes in high and low SPAG6 expression group. (E-H) GSEA of *SPAG6*. –, no statistical significance; *, P<0.05; ****, P<0.0001. THCA, thyroid carcinoma; HR, hazard ratio; CI, confidence interval; GSEA, gene set enrichment analysis.

Our results also show gender-specific differences, with high *SPAG6*-expression cancers being more prevalent in women (e.g., ACC) and low *SPAG6*-expression cancers being more common in men (e.g., GBM, GBMLGG, and LUSC). The Human Protein Atlas indicates SPAG6 expression in various tissues, including the brain, respiratory system, male tissues, and female tissues, although the level of expression varies between males and females, providing insights into gender-specific cancer diagnosis.

SPAG6 expression is associated with prognosis in various cancers. High *SPAG6* expression is linked to better survival in LAML and ALL, while low expression is associated with poor prognosis in TGCT. These findings suggest *SPAG6* as a potential prognostic biomarker. In hematologic cells, *SPAG6* regulates proliferation and apoptosis and can be targeted therapeutically through the P53 pathway (33). Our study is the first to examine *SPAG6* in THCA and to report that it is involved in DNA repair, MYC targets, peroxisome, and G2M checkpoint, but further experimental validation is needed to clarify the mechanism underlying this relationship.

SPAG6 expression is also associated with important biomarkers such as TMB, MSI, and tumor ploidy, which are crucial in predicting the response to immunotherapy (34). The expression of *SPAG6* can serve as a guide for immunotherapy in different types of cancer. Additionally, our study revealed a link between *SPAG6* expression and genetic heterogeneity, including DNA mutations and RNA modifications, particularly in BLCA. Contrary to previous findings, we observed that lower *SPAG6* expression was associated with higher stemness in tumors, indicating its facilitative role in cancer development (35). These findings highlight the significance of *SPAG6* in cancer progression and provide insights for potential therapeutic approaches.

In addition, immunotherapy has been shown to provide durable responses in some clinical patients, but only a small percentage of individuals respond to the treatment. A study has shown that increasing immunogenicity by modifying the TME can resolve these issues (36). Our study found a positive association between *SPAG6* expression and immune score, stromal score, and ESTIMATE score in various cancers. The presence and function of immune cells in the TME are crucial for antitumor immunity, and TME heterogeneity affects treatment response and clinical outcomes (37-39). Our investigation confirmed the positive relationship between cancer and *SPAG6* expression, as observed in the study regarding B cells and DCs (11). The correlation between *SPAG6* expression and various immunomodulators, including chemokines, receptors, MHCs, immune inhibitors, and immunostimulators, was also evaluated. *SPAG6* expression is closely linked to immune cell infiltration in the TME, impacting cancer immunotherapy and the need to shift the TME from a tolerogenic state to an immunogenic one. The study supports the role of *SPAG6* in tumor immunotherapy by revealing its relationship with immune checkpoint genes. *SPAG6* expression was positively associated with a successful response in most cancers, indicating its potential as an immune checkpoint. If the role of SPAG6 in the initiation and progression of THCA and its relationship with prognosis can be demonstrated, it could be considered a promising target for new drugs against this tumor. These results show that a quest for greater precision in molecular analysis could be the key to greater precision in personalized medicine.

However, the effects of immunotherapy are complex and are influenced by multiple and specific factors in each cancer. This is a limitation of our study and requires further *in vivo* experiments and clinical observations for the role of *SPAG6* in tumorigenesis and progression to be fully understood. Despite these limitations, our findings provide a foundation for future studies on *SPAG6* in the development and treatment of cancers, especially THCA.

Conclusions

In conclusion, this study found that the expression level of *SPAG6* was differentially expressed in various cancers at different tumor stages and grades, with gender-associated expression observed in certain cancers. The variation in *SPAG6* expression between progression and survival suggests its prognostic value in cancer. The results indicate that *SPAG6* affects immune infiltration, regulates the TME, and plays a role in the development of cancers. Additionally, *SPAG6* was positively correlated with a successful tumor therapy and may be a potential immune checkpoint.

Acknowledgments

Funding: This study was funded by Taishan Scholars Program of Shandong Province (No. ts20130913), National Natural Science Foundation of China (No. 82171150), and the National Natural Science Foundation of Shandong Province (No. ZR2020MH179).

Footnote

Reporting Checklist: The authors have completed the MDAR reporting checklist. Available at https://gs.amegroups.com/article/view/10.21037/gs-24-157/rc

Data Sharing Statement: Available at https://gs.amegroups.com/article/view/10.21037/gs-24-157/dss

Peer Review File: Available at https://gs.amegroups.com/article/view/10.21037/gs-24-157/prf

Conflicts of Interest: All authors have completed the ICMJE uniform disclosure form (available at https://gs.amegroups.com/article/view/10.21037/gs-24-157/coif). The authors have no conflicts of interest to declare.

Ethical Statement: The authors are accountable for all aspects of the work in ensuring that questions related to the accuracy or integrity of any part of the work are appropriately investigated and resolved. The studies involving human samples were approved by the Shandong Provincial ENT Hospital Ethical Committee (No. 2024-019-01). Written informed consent to participate in this study was provided by the participants. The study was conducted in accordance with the Declaration of Helsinki (as revised in 2013).

References

1. Du T, Gao J, Li P, et al. Pyroptosis, metabolism, and tumor immune microenvironment. Clin Transl Med 2021;11:e492.
2. Priestley P, Baber J, Lolkema MP, et al. Pan-cancer whole-genome analyses of metastatic solid tumours. Nature 2019;575:210-6.
3. Siliņa K, Zayakin P, Kalniņa Z, et al. Sperm-associated antigens as targets for cancer immunotherapy: expression pattern and humoral immune response in cancer patients. J Immunother 2011;34:28-44.
4. Yang P, Meng M, Zhou Q. Oncogenic cancer/testis antigens are a hallmarker of cancer and a sensible target for cancer immunotherapy. Biochim Biophys Acta Rev Cancer 2021;1876:188558.
5. Kulkarni P, Shiraishi T, Rajagopalan K, et al. Cancer/testis antigens and urological malignancies. Nat Rev Urol 2012;9:386-96.
6. Zheng DF, Wang Q, Wang JP, et al. The Emerging Role of Sperm-Associated Antigen 6 Gene in the Microtubule Function of Cells and Cancer. Mol Ther Oncolytics 2019;15:101-7.
7. Li X, Xu L, Sun G, et al. Spag6 Mutant Mice Have Defects in Development and Function of Spiral Ganglion Neurons, Apoptosis, and Higher Sensitivity to Paclitaxel. Sci Rep 2017;7:8638.
8. Li X, Xu L, Li J, et al. Otitis media in sperm-associated antigen 6 (Spag6)-deficient mice. PLoS One 2014;9:e112879.
9. Sapiro R, Kostetskii I, Olds-Clarke P, et al. Male infertility, impaired sperm motility, and hydrocephalus in mice deficient in sperm-associated antigen 6. Mol Cell Biol 2002;22:6298-305.
10. Bao Z, Zhu R, Fan H, et al. Aberrant expression of SPAG6 and NM23 predicts poor prognosis of human osteosarcoma. Front Genet 2022;13:1012548.
11. Wu Q, Yan Y, Shi S, et al. DNMT3b-mediated SPAG6 promoter hypermethylation affects lung squamous cell carcinoma development through the JAK/STAT pathway. Am J Transl Res 2022;14:6964-77.
12. Altenberger C, Heller G, Ziegler B, et al. SPAG6 and L1TD1 are transcriptionally regulated by DNA methylation in non-small cell lung cancers. Mol Cancer 2017;16:1.
13. Zhang R, Zhu H, Yuan Y, et al. SPAG6 promotes cell proliferation and inhibits apoptosis through the PTEN/PI3K/AKT pathway in Burkitt lymphoma. Oncol Rep 2020;44:2021-30.
14. Zhao B, Yin J, Ding L, et al. SPAG6 regulates cell proliferation and apoptosis via TGF-β/Smad signal pathway in adult B-cell acute lymphoblastic leukemia. Int J Hematol 2024;119:119-29.
15. Yi M, Zheng X, Niu M, et al. Combination strategies with PD-1/PD-L1 blockade: current advances and future directions. Mol Cancer 2022;21:28.
16. Wu Q, Jiang L, Li SC, et al. Small molecule inhibitors targeting the PD-1/PD-L1 signaling pathway. Acta Pharmacol Sin 2021;42:1-9.

17. Bialek-Waldmann JK, Domning S, Esser R, et al. Induced dendritic cells co-expressing GM-CSF/IFN-α/tWT1 priming T and B cells and automated manufacturing to boost GvL. Mol Ther Methods Clin Dev 2021;21:621-41.
18. Jhunjhunwala S, Hammer C, Delamarre L. Antigen presentation in cancer: insights into tumour immunogenicity and immune evasion. Nat Rev Cancer 2021;21:298-312.
19. Cooley LF, El Shikh ME, Li W, et al. Impaired immunological synapse in sperm associated antigen 6 (SPAG6) deficient mice. Sci Rep 2016;6:25840.
20. Liu J, Lichtenberg T, Hoadley KA, et al. An Integrated TCGA Pan-Cancer Clinical Data Resource to Drive High-Quality Survival Outcome Analytics. Cell 2018;173:400-416.e11.
21. Malta TM, Sokolov A, Gentles AJ, et al. Machine Learning Identifies Stemness Features Associated with Oncogenic Dedifferentiation. Cell 2018;173:338-354.e15.
22. Zeng D, Ye Z, Shen R, et al. IOBR: Multi-Omics Immuno-Oncology Biological Research to Decode Tumor Microenvironment and Signatures. Front Immunol 2021;12:687975.
23. Li T, Fan J, Wang B, et al. TIMER: A Web Server for Comprehensive Analysis of Tumor-Infiltrating Immune Cells. Cancer Res 2017;77:e108-10.
24. Thorsson V, Gibbs DL, Brown SD, et al. The Immune Landscape of Cancer. Immunity 2019;51:411-2.
25. Elhanani O, Ben-Uri R, Keren L. Spatial profiling technologies illuminate the tumor microenvironment. Cancer Cell 2023;41:404-20.
26. Chen P, Hsu WH, Han J, et al. Cancer Stemness Meets Immunity: From Mechanism to Therapy. Cell Rep 2021;34:108597.
27. Barretina J, Caponigro G, Stransky N, et al. The Cancer Cell Line Encyclopedia enables predictive modelling of anticancer drug sensitivity. Nature 2012;483:603-7.
28. Mehnert JM, Varga A, Brose MS, et al. Safety and antitumor activity of the anti-PD-1 antibody pembrolizumab in patients with advanced, PD-L1-positive papillary or follicular thyroid cancer. BMC Cancer 2019;19:196.
29. Lorch J, Barletta J, NehsM, et al. A phase II study of nivolumab (N) plus ipilimumab (I) in radioidine refractory differentiated thyroid cancer (RAIR DTC) with exploratory cohorts in anaplastic (ATC) and medullary thyroid cancer (MTC). J Clin Oncol 2020;38:abstr 6513.
30. Mulaw MA, Krause A, Deshpande AJ, et al. CALM/AF10-positive leukemias show upregulation of genes involved in chromatin assembly and DNA repair processes and of genes adjacent to the breakpoint at 10p12. Leukemia 2012;26:1012-9.
31. Jiang M, Chen Y, Deng L, et al. Upregulation of SPAG6 in Myelodysplastic Syndrome: Knockdown Inhibits Cell Proliferation via AKT/FOXO Signaling Pathway. DNA Cell Biol 2019;38:476-84.
32. Mijnes J, Tiedemann J, Eschenbruch J, et al. SNiPER: a novel hypermethylation biomarker panel for liquid biopsy based early breast cancer detection. Oncotarget 2019;10:6494-508.
33. Yang B, Wang L, Luo X, et al. SPAG6 silencing inhibits the growth of the malignant myeloid cell lines SKM-1 and K562 via activating p53 and caspase activation-dependent apoptosis. Int J Oncol 2015;46:649-56.
34. Addeo A, Friedlaender A, Banna GL, et al. TMB or not TMB as a biomarker: That is the question. Crit Rev Oncol Hematol 2021;163:103374.
35. Friedmann-Morvinski D, Verma IM. Dedifferentiation and reprogramming: origins of cancer stem cells. EMBO Rep 2014;15:244-53.
36. Murciano-Goroff YR, Warner AB, Wolchok JD. The future of cancer immunotherapy: microenvironment-targeting combinations. Cell Res 2020;30:507-19.
37. Fujii SI, Shimizu K. Immune Networks and Therapeutic Targeting of iNKT Cells in Cancer. Trends Immunol 2019;40:984-97.
38. Efimova I, Catanzaro E, Van der Meeren L, et al. Vaccination with early ferroptotic cancer cells induces efficient antitumor immunity. J Immunother Cancer 2020;8:e001369.
39. Junttila MR, de Sauvage FJ. Influence of tumour microenvironment heterogeneity on therapeutic response. Nature 2013;501:346-54.

Cite this article as: Li X, Wang Y, Li X, Kong L, Díez JJ, Wang H, Zhang D. A comprehensive pan-cancer analysis revealing *SPAG6* as a novel diagnostic, prognostic and immunological biomarker in tumor. Gland Surg 2024;13(6):999-1015. doi: 10.21037/gs-24-157